https://doi.org/10.5194/essd-2025-569
Preprint. Discussion started: 12 May 2026

Open Access Earth System Science Data Discussions

PolarLakes: A Bi-Weekly Dataset of Supraglacial Lakes on Antarctic Ice Shelves from Multi-Sensor Satellite Observations (2015–2024)

Celia A. Baumhoer[1], Jonas Koehler[1,2], Bert Wouters[3], Stef Lhermitte[3,4], Andreas J. Dietz[1] and Claudia Kuenzer[1,5]

[1]Land Surface Dynamics Department, German Remote Sensing Data Center (DFD), German Aerospace Center (DLR), Wessling, D-82234, Germany
[2]Department of Glaciology and Climate, Geological Survey of Denmark and Greenland (GEUS), Copenhagen, DK-1350, Denmark
[3]Department of Geoscience & Remote Sensing, University of Technology, Delft, NL-2628, Netherlands
[4]Department of Earth & Environmental Sciences, Ku Leuven, Leuven, BE-3001, Belgium
[5]Institute for Geography and Geology, University of Wuerzburg, D-97074 Wuerzburg, Germany

Correspondence to: Celia A. Baumhoer (celia.baumhoer@dlr.de)

Abstract. Supraglacial lakes in Antarctica are key indicators of surface meltwater processes and play a significant role in ice shelf stability and ice sheet dynamics. Despite their importance, the understanding of their spatiotemporal dynamics remains limited due to their high variability and the lack of consistent, large-scale monitoring approaches. To date, no bi-weekly, pan-Antarctic dataset exists that captures supraglacial lake extent over recent years. To address this gap, we introduce the PolarLakes dataset, generated using a deep learning-based workflow that automates the detection and mapping of supraglacial lakes across Antarctic ice shelves. This method integrates Sentinel-1 synthetic aperture radar (SAR) and Sentinel-2 optical imagery to enhance spatial and temporal coverage while improving detection accuracy under challenging conditions such as cloud cover and surface refreezing. The resulting open-access dataset provides bi-weekly records of supraglacial lake extents at 10 meter spatial resolution from 2015 through 2024. It reveals extensive ponding in East Antarctica until a pan-Antarctic peak in lake area in 2020, followed by higher melt extents on the Antarctic Peninsula, culminating in a secondary peak on the Antarctic Peninsula in 2023. The PolarLakes dataset offers a valuable resource for investigating supraglacial hydrology and provides essential observational constraints for hydrological and ice sheet modeling. The PolarLakes dataset is available at DLR's GeoService at https://geoservice.dlr.de/web/datasets/polarlakes.

Short Summary.

PolarLakes is a new open dataset tracking meltwater lakes on Antarctic ice shelves every two weeks from 2015–2024. Using AI and satellite data from different sensors the monitoring of lakes is improved even during cloudy conditions. The record shows significant variations in ponding and lake formation, with a continent-wide peak occurring in 2020 within the observed period. To end, the PolarLakes dataset helps us to better understand the dynamics of surface hydrology in Antarctica.

https://doi.org/10.5194/essd-2025-569
Preprint. Discussion started: 12 May 2026

Open Access Earth System Science Data Discussions

1 Introduction

Supraglacial lakes are surface water bodies that form on ice sheets and glaciers due to meltwater accumulation during periods of enhanced surface melting (Arthur et al., 2020). In Antarctica, particularly across the ice shelves and coastal margins of the Antarctic Ice Sheet, these lakes have gained increasing scientific attention in recent decades (Arthur et al., 2022; Corr et al., 2022; Dell et al., 2024; Stokes et al., 2019). Once considered relatively rare due to the continent's cold and dry climate, satellite observations have revealed widespread and seasonally dynamic networks of supraglacial lakes, especially during austral summer months (Arthur et al., 2022; Dirscherl et al., 2021b). Supraglacial lakes have now been observed in vast numbers across coastal regions of East Antarctica (Mahagaonkar et al., 2024; Stokes et al., 2019), West Antarctica, and the Antarctic Peninsula (AP) (Corr et al., 2022), especially on low-elevation ice shelves. The presence of supraglacial lakes has direct implications for the structural integrity of ice shelves (Stokes et al., 2019). When meltwater collects in surface depressions and crevasses, it can drive fracturing through hydrofracture processes, which may ultimately result in the sudden collapse of ice shelves (Lai et al., 2020; Leeson et al., 2020). These collapse events have the potential to accelerate the flow of upstream grounded ice into the ocean, thereby potentially enhancing Antarctica's contribution to global sea-level rise by reducing ice shelf buttressing forces (Fürst et al., 2016). Additionally, supraglacial lakes influence the surface energy balance through lowering surface albedo by replacing high reflective snow and ice by water. This self-reinforcing melt-albedo feedback enhances solar energy absorption and accelerates surface melt (Dell et al., 2024). Supraglacial lake drainage is known to accelerate grounded ice flow on the AP (Scambos et al., 2004; Tuckett et al., 2019) but it still remains unclear whether similar drainage affects ice dynamics in West and East Antarctica by reaching the bed and altering basal conditions (Arthur et al., 2020).

Despite typically covering only a small fraction of the Antarctic surface, supraglacial lakes are crucial to monitor because of their sensitivity to climate variability and their role in ice shelf dynamics. Their distribution and seasonal evolution are shaped by a combination of air temperature, solar radiation, wind conditions, and atmospheric modes which vary spatially and temporally across different regions of Antarctica (Dirscherl et al., 2021b; Mahagaonkar et al., 2024). As surface melt intensifies under projected future warming scenarios (Trusel et al., 2015), supraglacial lake formation is expected to expand further inland and across higher elevations, raising concerns over the long-term stability of Antarctic ice shelves. Consequently, mapping and monitoring these lakes is crucial for understanding their seasonal variations and impacts on ice shelf stability, as well as for predicting future changes in ice sheet dynamics in response to global warming. Large-scale supraglacial lake mapping efforts provide essential input for ice sheet models and help to identify regions of meltwater production (Bell et al., 2018). Their distribution and dynamics offer valuable insights into surface melt processes, ice shelf stability, and potential implications for sea-level rise.

The monitoring of supraglacial lake dynamics has evolved with the availability in open access satellite imagery, enabling researchers to monitor these features with unprecedented temporal and spatial resolution. First lakes were reported by Mellor and McKinnon (1960) on Amery Ice Shelf, followed by publications observing supraglacial lakes on ice shelves before their

https://doi.org/10.5194/essd-2025-569
Preprint. Discussion started: 12 May 2026

disintegration on Prince Gustav, Larsen A and Wilkins ice shelves. In 2000, Scambos et al. (2000) suggested for the first time the instability of ice shelves due to supraglacial lake formation. With increasing availability of medium resolution satellite imagery on a higher temporal scale (starting with the availability of Landsat 8 imagery), the number of publications on supraglacial lake formation increased significantly (Arthur et al 2020). Methods for Antarctic supraglacial lake detection range from visual interpretation of images (Mellor Mc Kinnon 1960), manual delineation, band ratios and indices (Corr et al., 2022; Moussavi et al., 2020; Stokes et al., 2019) to the use of machine and deep learning methods (Dell et al., 2024; Dirscherl et al., 2021a). The large-scale application of band ration and machine learning techniques resulted in the open access supraglacial lake datasets listed in Table 1. These datasets are mostly based on the method developed by Moussavi et al. (2020) or modified versions of it, which uses thresholding of the NDWI (Normalized Differential Water Index) and NDSI (Normalized Differential Snow Index) in combination with thresholding additional TOA Reflectance and brightness temperature values from Landsat bands 2 and 6. This makes the method straightforward to implement and upscaling for large-scale processing is easily possible. The workflow has been applied to Landsat-8 and Sentinel-2 satellite data resulting in datasets ranging from 2014 until 2021 (Arthur et al., 2022; Corr et al., 2022; Mahagaonkar et al., 2024). Additionally, different machine learning based methods were developed by Dell et al. (2022) for Landsat-8 imagery and Dirscherl et al. (2020, 2021a) for Sentinel-1 and Sentinel-2 data. The dataset published by Dell et al. (2024) provides monthly supraglacial dynamics during the time period 2014 until 2021 for all major Antarctic ice shelves. Dirscherl et al. (2021b) used their methodology to create a bi-weekly dataset for six selected ice shelves for the time period 2015-2021. Currently available pan-Antarctic open-access datasets rely primarily on optical imagery from Landsat-8 and Sentinel-2, but they provide no coverage beyond 2021 and are limited to a maximum consistent temporal resolution of one observation per month and a spatial resolution of 30 m.

Table 1 Existing large-scale and open access datasets of Antarctic supraglacial lakes listed by publication date.

Study	Spatial coverage	Time span	Temporal resolution	Satellite data	Delineation method	Dataset DOI
Stokes et al. 2019	EAIS	January 2017	-	Landsat-8/ Sentinel-2	NDWI thresholding	-
Moussavi et al. 2020	most important ice shelves	2014-2020	16-days/ L8 scenes	Landsat-8	NDWI/NDSI thresholding	10.15784/601401
Dirscherl et al. 2021b	six ice shelves	2015-2021	bi-weekly	Sentinel-2/ Sentinel-1	Random Forest, U-Net	-
Corr et al. 2022	WAIS, AP	January 2017	-	Landsat-8/ Sentinel-2	Modified Moussavi	10.5281/zenodo.5642755
Arthur et al. 2022	EAIS	2014-2020	January each year	Landsat 8	Moussavi	10.5285/a9f2e4b5-9c2e-4ea5-8c0c-db5f6585128a
Dell et al. 2024	most important ice shelves	2014-2021	monthly	Landsat-8	Clustering, Random Forest	10.17863/CAM.108421
Mahagaonkar et al. 2024	Dronning Maud Land	2014-2021	L8/S2 scenes	Landsat-8/ Sentinel-2	Moussavi	10.21334/NPOLAR.2023.31AAE21F

This study aims to extend the open access dataset availability to a more recent period and to enhance the temporal and spatial resolution of Antarctic supraglacial lake datasets. The result is the novel bi-weekly dataset *PolarLakes* providing information

https://doi.org/10.5194/essd-2025-569
Preprint. Discussion started: 12 May 2026

on supraglacial lake dynamics derived from advanced optical and SAR satellite data over the current Sentinel era, spanning the years 2015 through 2024. Utilizing a combined deep learning approach for Sentinel-1 and Sentinel-2 data, we achieve reliable lake mapping even under challenging conditions like cloud cover and surface melt. The PolarLakes dataset provides high resolution information on recent supraglacial lake dynamics giving insights on critical hydrological processes, offering opportunities for improved ice sheet modelling efforts. In the end, our research will provide critical insights into the influence of supraglacial lakes on the stability of ice shelves.

2 Methods

The PolarLakes dataset is generated through a multi-step workflow (Figure 1) that combines optical and SAR satellite data. Pre-processing prepares Sentinel-2 and Sentinel-1 imagery, which are then classified using two separately trained U-Net architectures to detect supraglacial lakes. Post-processing enhances reliability by applying topographical masks and removing detections beyond the Antarctic coastline. The resulting predictions are aggregated into bi-weekly binary layers, representing maximum lake extents during each two-week period of the austral summer. Lake recurrence is subsequently calculated, and the final dataset includes georeferenced raster files, summary statistics, and scientific plots. A detailed description of each workflow component is provided below.

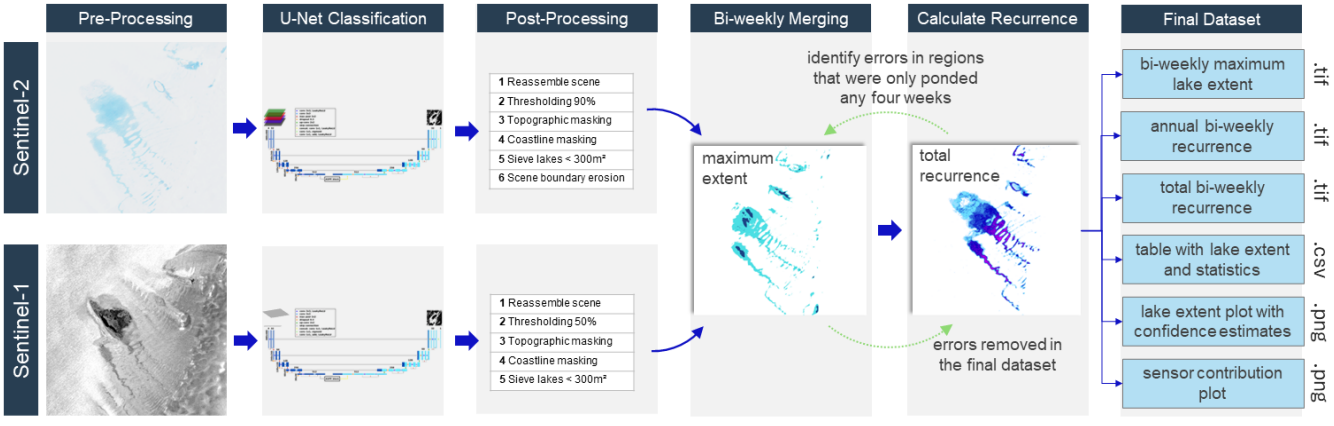

Figure 1 Workflow for the PolarLakes dataset generation, including satellite data pre-processing, deep learning classification with U-Net, post-processing for quality enhancement, temporal merging of bi-weekly maximum extents, recurrence calculation, and final dataset components.

2.1 Satellite Data Pre-Processing

The PolarLakes dataset covers 22 ice shelves experiencing frequent surface melt (see Figure 2 for ice shelves included in the dataset). For every ice shelf, we established a region of interest and gathered all accessible Sentinel-1 scenes and all Sentinel-2 images with cloud coverage below 75 % during the months of November through March. We accessed the data from the Sentinel Long Term Archive (S-LTA) hosted by the German Aerospace Center and pre-processed the data as explained below.

https://doi.org/10.5194/essd-2025-569
Preprint. Discussion started: 12 May 2026

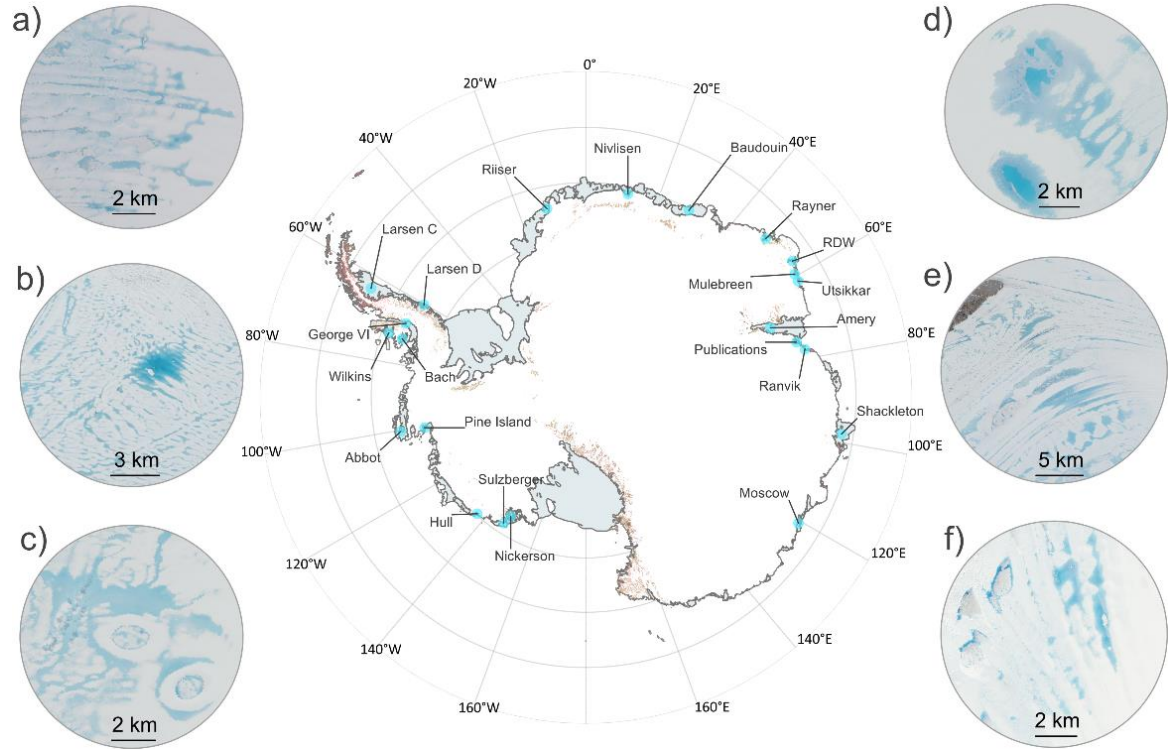

Figure 2 Map of Antarctic ice shelves included in the PolarLakes dataset. Insets highlight examples of supraglacial lake formation during periods of intense surface melt, with panels showing extensive ponding on the (a) Larsen C Ice Shelf on 13 January 2023, (b) George VI Ice Shelf on 19 January 2020, (c) Bach Ice Shelf on 15 January 2025, (d) Riiser-Larsen Ice Shelf on 24 January 2017, (e) Amery Ice Shelf 27 January 2017, and (f) Moscow University Ice Shelf on 27 January 2020. RDW: Robert/Downer/Wilma. Copernicus Sentinel-2 Data 2025.

2.1.1 Sentinel-1

The supraglacial lake detection from radar data is based on 20,250 Sentinel-1 IW single polarized HH scenes with a spatial resolution of 10 m. The Level-1 GRD (Ground Range Detected) Sentinel-1 products require further pre-processing to retrieve georeferenced and terrain corrected imagery. The basic pre-processing steps include updating the orbit metadata with the "Apply Orbit File" function. Afterwards, thermal noise is removed in all sub-swaths to enhance image data quality. The next step involves radiometric calibration in order to retrieve the backscattering coefficient, denoted as sigma naught (σ0). Radiometric calibration is essential for ensuring that backscatter signals are comparable across different acquisitions, sensors, and observation conditions. It enables the conversion of raw digital numbers into physically meaningful values, allowing consistent interpretation of surface properties. In addition to this, speckle filtering was applied to mitigate noise. Finally, the satellite scenes are corrected for any terrain distortions based on the TanDEM-X Polar DEM 90 (Wessel et al., 2021) during terrain correction. All processing steps were performed with the Graph Processing Tool (GPT) of the ESA SNAP Software 8.0.5. (SNAP, 2020).

https://doi.org/10.5194/essd-2025-569
Preprint. Discussion started: 12 May 2026

2.2 Sentinel-2

For the PolarLakes dataset 25,772 Sentinel-2 L1C satellite scenes were pre-processed. We selected all available scenes over the defined AOIs with an assigned cloud coverage less than 75 %. The Sentinel-2 pre-processing is similar to (Koehler et al., 2025) and summarized in the following: First, Sentinel-2 L1C data which is atmospherically corrected to achieve L2A Bottom-Of-Atmosphere (BOA) reflectance utilizing the Sen2Cor processor (Sen2Cor 2.11.00 Software Release Note). Digital numbers (DN) are transformed into reflectance values by applying the corresponding scaling factors and offsets associated with the specific processing baseline of the product. Minor instances of two to four pixels with no data values introduced to the cloud masking algorithm within the image acquisition strip of the scene are addressed through spatial interpolation. For the final datasets, image stacks are constructed that encompass the spectral bands in the visible green and red (Sentinel-2 bands 3 and 4), in addition to the Soil/Water Index (SWI) (Dirscherl et al., 2020) and the Automated Water Extraction Index (AWEInsh) (Feyisa et al., 2014). These specific bands and indices are chosen as prior research indicated their substantial predictive usefulness for SGL detection (Dirscherl et al., 2020). Furthermore, and empirical analyses demonstrated that the AWEInsh, in particular, mitigated misclassifications in regions characterized by topographic shadows, whereas the SWI proved advantageous for differentiating rocks and moraines from surface water (Koehler et al., 2025). The shortwave infrared bands (SWIR1 and SWIR2) are resampled for indices calculation to correspond with the 10 m resolution of bands 3 and 4.

2.3 U-Net Supraglacial Lake Detection

The supraglacial lake detection methodology applied in this study is based on the approach developed by Dirscherl et al. (2021), originally designed for Sentinel-1 SAR imagery using HH-polarized data. We adopt the same model architecture, training data and training procedure to create trained weights for Sentinel-1 data. To extend the methodology to optical data, we train a modified version of the network separately with four input channels for use with Sentinel-2 imagery.

2.3.1 Training and Validation Data

For Sentinel-1, the dataset includes image tiles covering periods of pronounced surface melt between 2016 and 2020, focusing on the austral summer months (1 December to 1 March). The data spans a broad range of Antarctic environments - covering eight sites on the East Antarctic Ice Sheet (EAIS), two on the West Antarctic Ice Sheet (WAIS), and three on the AP - capturing various surface types including bare and blue ice, wet and dry snow, slush, crevasse fields, rock outcrops, and supraglacial lakes. Ground truth labels for Sentinel-1 scenes are manually created for the classes "water" and "non-water", using Sentinel-2 supraglacial lake extent mapping products for support. These products were developed by training a RF classifier on optical Sentinel-2 and TanDEM-X topographic data (Dirscherl et al., 2020). However, comparisons between Sentinel-2 maximum lake extents and lake boundaries visible in Sentinel-1 imagery revealed significant differences, likely due to varying acquisition times, data availability, and the impact of wind or freezing on lake visibility in SAR imagery compared to optical imagery. Hence, the architecture is only able to be trained to detect open surface water lakes that are not impacted by slush, wind

https://doi.org/10.5194/essd-2025-569
Preprint. Discussion started: 12 May 2026

Open Access Earth System Science Data Discussions

roughening or thin ice layers on top. A total of 21,200 tiles were obtained from the labelled Sentinel-1 imagery by tiling it at 480 x 480 pixels, with a 200-pixel overlap, and augmenting it 12 times by rotating and flipping, in order to artificially increase the training data.

For Sentinel-2 model training, we use 16 scenes with 33 manually defined training regions to represent the full diversity of lake and non-lake surface features especially including difficult features such as slush, shallow and elongated lakes, shadow and blue ice. The labeling follows the supraglacial lake labelling ruleset published by Baumhoer and Koehler (2025) to ensure a consistent labeling strategy. In total, 3,420 labeled Sentinel-2 tiles are created by patch tiling with a 100-pixel overlap using 480 × 480 pixel patches and 12-time augmentation as well. Training regions for Sentinel-2 and Sentinel-1 imagery are depicted in Figure 3. To cover the most diverse appearance of lakes and lake-like features for optical and SAR data we decided to select the locations for training and test data for each sensor independently considering image availability and lake occurrence.

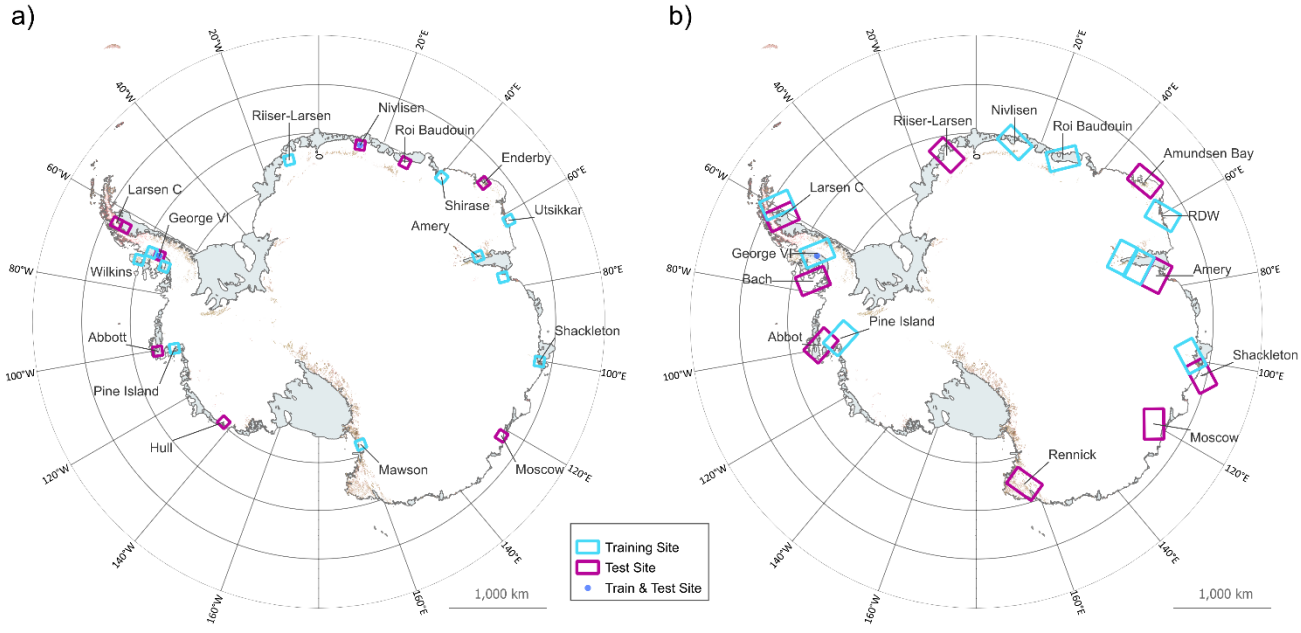

Figure 3 Spatial distribution of training and test sites for Sentinel-2 (a) and Sentinel-1 (b) data. Modified after Dirscherl et al. (2021a) and Koehler et al. (2025). RDW: Robert/Downer/Wilma

2.3.2 Network Architecture

We implement a modified U-Net architecture for supraglacial lake segmentation as described in Dirscherl et al. (2021a). The network is based on a fully convolutional encoder-decoder design, extended with residual connections and an Atrous Spatial Pyramid Pooling (ASPP) module to improve feature representation across multiple spatial scales. The architecture consists of four downsampling and four upsampling blocks, each composed of two 3×3 convolutions with padding, LeakyReLU activation, residual connections via 1×1 convolutions, 2×2 max pooling, and a dropout rate of 0.3 to prevent overfitting. The encoder doubles the number of feature channels per block, reaching a maximum of 512. At the bottleneck, an ASPP module

https://doi.org/10.5194/essd-2025-569
Preprint. Discussion started: 12 May 2026

with dilation rates of 2, 4, 8, and 12 captures multi-scale spatial context, aiding the detection of SGLs with variable size and shape. The decoder mirrors the encoder structure and incorporates skip connections to preserve high-resolution spatial detail. A final 1×1 convolution followed by a sigmoid activation generates a per-pixel probability map of lake presence. For Sentinel-2 data the same model architecture was used except with the modification to allow four input channels, instead of one. Train validation split for training was set to 80 to 20 %. For each satellite sensor individual model weights were trained using binary crossentropy as loss function and the Adamax optimizer with an initial learning rate of 0.001, reduced by a factor of 0.1 after three epochs of stagnant validation loss, down to a minimum of 0.0000001 for Sentinel-2 and 0.0001 for Sentinel-1. The final model, consisting of approximately 10.6 million trainable parameters, converged after 25 epochs for Sentinel-2 and 30 epochs for Sentinel-1 data.

2.4 Post-Processing

During post-processing the individual 480 x 480 pixel patches are reassembled. In overlapping areas, the average prediction probability is calculated. The prediction probabilities are thresholded by 50 % for Sentinel-1 and 90 % for Sentinel-2 to create binary supraglacial lake maps. The thresholds are chosen empirically for each satellite sensor individually as this results in highest overall accuracies compared to higher or lower thresholds. Furthermore, areas with slopes steeper than 5 % and altitudes over 1,500 m were masked based on the TanDEM-X Polar DEM 90 (Wessel et al., 2021) as lake appearance in these regions is very unlikely (Stokes et al., 2019). The seaward boundary of lakes on ice shelves is masked with the coastline of the IceLines dataset (Baumhoer et al., 2023). Finally, lakes smaller than three pixels (~300 m^2) are removed to reduce clutter. In Sentinel-2 imagery, false classifications exist along the scene borders. In order to remove these, we use the individual scene extents of each scene and erode the prediction probability raster layer by ten pixels. This successfully removes scene border artifacts in the final dataset without removing relevant lake predictions.

2.5 Dataset compilation

2.5.1 Selection of ice shelves

The final PolarLakes dataset includes 22 individual ice shelves (see Figure 2) covering almost the entire surface melt observed on Antarctic ice shelves. To select the most important ice shelves for our dataset, we used existing supraglacial lake datasets for Antarctica from January 2017 (Corr et al., 2022; Stokes et al., 2019) and intersected the lake area with ice shelf polygons from the Antarctic Digital Database (Antarctic Digital Database, 2020). We selected all shelves larger than 100 km^2 with an intersection area > 1 km^2 and a lake percentage coverage relative to the ice shelf size of > 0 %. From the identified 19 shelves we had to exclude Ross Ice Shelf due to limited data coverage of Sentinel-2. From further existing studies (Arthur et al., 2022; Dell et al., 2024) we identified four additional ice shelves that experienced frequent ponding after 2017 and added them to the PolarLakes dataset – namely Abbot, Larsen C, Publications and Robert/Downer/Wilma. In total, the 22 ice shelves cover 98.6 % of the ponded area on pan-Antarctic ice shelves observed in January 2017.

https://doi.org/10.5194/essd-2025-569
Preprint. Discussion started: 12 May 2026

Open Access Earth System Science Data Discussions

2.5.2 Bi-weekly merging

For each selected ice shelf, we run the inference with the trained weights for all available Sentinel-1 and Sentinel-2 scenes available from the Sentinel long-term archive at the German Aerospace Center. For each two-week interval between November and March (austral summer) all available binary prediction results from Sentinel-1 and Setinel-2 are merged into a bi-weekly maximum extent. The two-week interval turned out to include a sufficient amount of available Sentinel-1 and Sentinel-2 data to create a consistent data product with uniform time steps at 10 m spatial resolution. For each season, a maximum of ten bi-weekly maximum extent layers is available, which is sometimes reduced due to limited scene availability. Per melt season, all maximum extents are summed to an annual recurrence dataset highlighting how often a lake occurred on a bi-weekly basis.

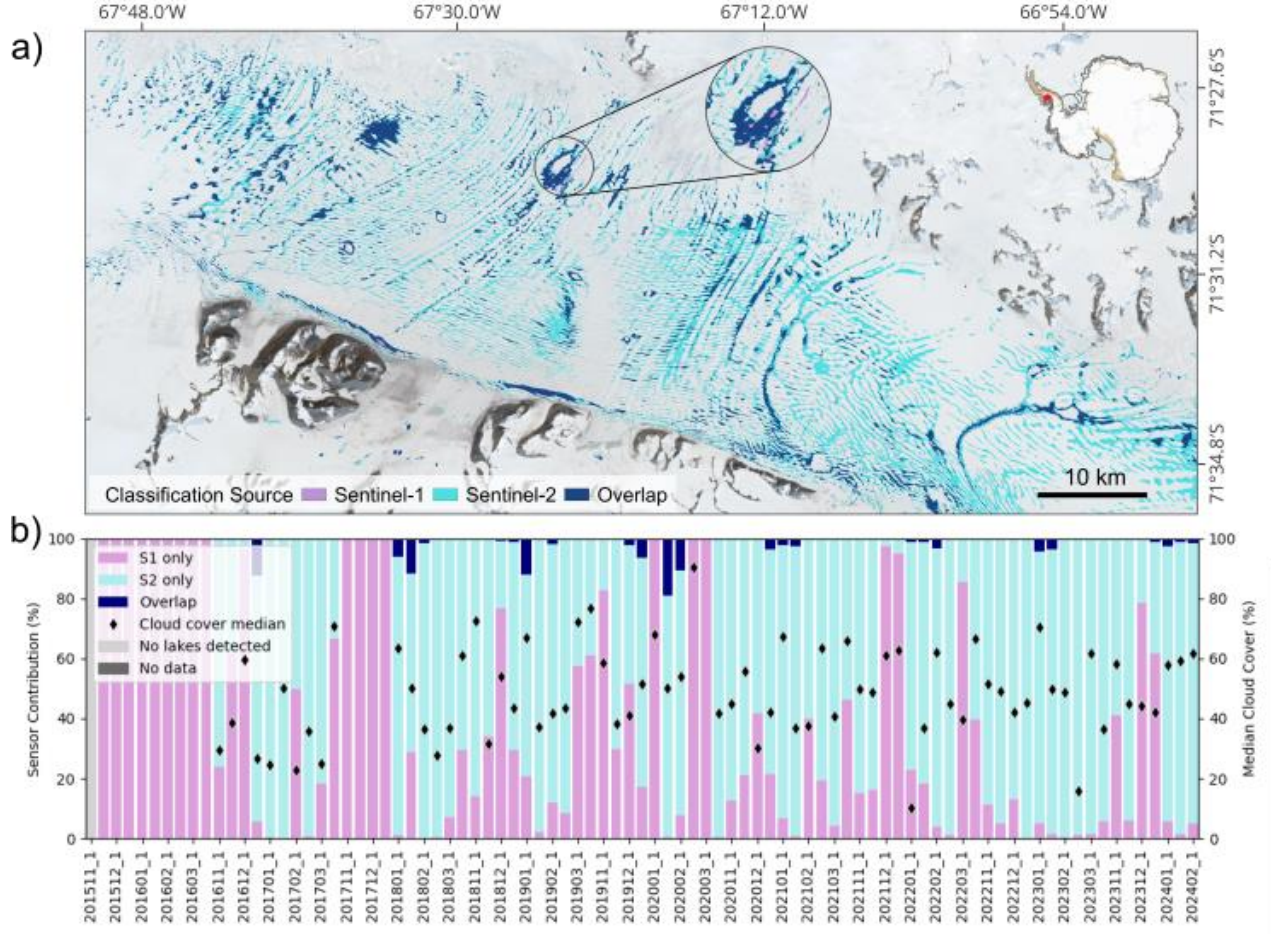

Figure 4 Satellite sensor sources for supraglacial lake classification. Panel (a) shows the spatial distribution of sensor sources used for lake classification on the George VI Ice Shelf during the second half of January 2020. Panel (b) displays the contribution of each sensor as a percentage for each bi-weekly classification result throughout the melt season. The median cloud cover for optical acquisitions (S2) is also shown as a reference for data quality. Modified after Dirscherl et al. (2022), contains Copernicus Sentinel-2 Data 2025.

https://doi.org/10.5194/essd-2025-569
Preprint. Discussion started: 12 May 2026

In general, most lake extents are detected using Sentinel-2 imagery, provided that there is low cloud cover. Only a small amount can be contributed using Sentinel-1 (see Figure 4 for the exact percentages of sensor contribution). An example of satellite sensor contribution to the classification result is given in Figure 4 for George VI Ice Shelf highlighting the considerably larger fraction of detections based on Sentinel-2 data. The supplementary material provides a full table with scene availability for each bi-weekly interval and each individual shelf. We deviate from this general merging approach only in the case of Pine Island Glacier. Here the Sentinel-1 imagery is very prone to misclassifications, likely due to very specific backscatter patterns in the firn, as visual inspection revealed. Therefore, the PolarLakes dataset only includes lake extents mapped from Sentinel-2 data for Pine Island Glacier.

2.5.3 Error reduction

Despite the networks being thoroughly trained, prediction errors remain. This can be mostly attributed to the fact that cloud detection algorithms in polar regions have a reduced performance due to the large underlying snow-covered areas. Therefore, the Sentinel-2 scene selection threshold of 75 % cloud cover provides only a rough estimate and fully cloud covered and shadowed scenes will end up in the inference from time to time. These scenes are often obscured by strong cloud shadows that can result in miss-classifications over large parts of the scene. Previous studies excluded false positives over e.g. cloud shadows manually (Arthur et al., 2022; Mahagaonkar et al., 2024) but we had to implement an automated approach due to the high number of processed scenes. We followed the stringent approach of Dell et al. (2024) to mask out errors introduced by clouds and cloud shadows by removing pixels classified as surface meltwater for two time steps or less (any two be-weekly intervals) throughout the entire study period.

3 Dataset Validation and Uncertainty Estimation

3.1 Accuracy Assessment based on Classification Performance

The classification performance for optical and SAR data is assessed separately for both sensors independently. This is necessary as no ground truth satellite scene exists for the bi-weekly merged maximum extent. The accuracy assessment is based on ten independent test sites from unique Sentinel-1 scenes and for Sentinel-2 on 16 sites covered extracted from 8 scenes. Exact locations of test sites for each sensor are shown in Figure 3. The accuracy assessment builds on the two original studies on the supraglacial lake mapping methods published in Dirscherl et al. (2021a) and Koehler et al. (2025) and hence follows different approaches.

For Sentinel-1, performance is assessed through point wise validation from manually labelled random points for "water" (supraglacial meltwater features) and "non-water" (remaining ice sheet surface features) features using Sentinel-1 imagery as the basis for manual labelling. Sentinel-2 maximum extent products from a Random Forest approach are only used as indicator for potential supraglacial lake occurrence (Dirscherl et al., 2020). Random point samples are created for the classified imagery, focusing on challenging discrimination areas and ensuring adequate sampling in potential misclassification regions by

https://doi.org/10.5194/essd-2025-569
Preprint. Discussion started: 12 May 2026

introducing a 250 m buffer around each water pixel. This results in 23,000 sample points within the buffered water class. The number of samples per scene is adjusted according to the proportion of classified lake pixels. A confusion matrix is generated, and accuracies computed for each specific test area (refer to Figure 5 for F1-Score). In total, the average Precision (88 %) and Recall (98 %) yielded an average F-score of 93 % for the "water" category, in contrast to the values of 99 %, 99 %, and 99 % for Precision, Recall, and F-score of the "non-water" category. This indicates, as soon as there is open water it will be very accurately detected with Sentinel-1 data.

The Sentinel-2 accuracy assessment is based on fully segmented ground-truth labels as common for accuracy assessments of CNN output. This approach better reflects the ability of a model to map spatially consolidated lake areas. Here, for all 16 test sites a pixel-wise comparison to the manual labels is performed to calculate the confusion matrix. In Figure 5, the F1-Score for each individual test region is shown and Table 2 summarizes precision, recall and F1-Score for each individual test site. The U-Net–derived lake masks show strong agreement with the reference data, yielding an overall F1-score of 0.91 with balanced precision and recall (both 0.91). Despite this high thematic accuracy, the derived lake area remains subject to uncertainty due to residual classification errors. Commission errors (≈0.09) may lead to overestimation of lake extent, whereas omission errors (≈0.09) may result in underestimation. These classification errors cannot be directly translated into a single quantitative measure of area uncertainty without spatially explicit error propagation. Furthermore, classification performance varies between test sites, reflecting differences in lake morphology and the presence of spectrally similar features (e.g., small, dark cloud cover in the Larsen C-1-2 region). Given balanced precision and recall, classification errors of approximately 9% suggest that lake area estimates may be affected by both over- and underestimation, though the net bias depends on class prevalence and spatial error distribution.

Visual examples of the prediction of the test data are given in the original method papers Dirscherl et al. (2021a) and Koehler et al. (2025). Additionally, we provide a visual overview of the detected lakes for sample regions in Figure 6.

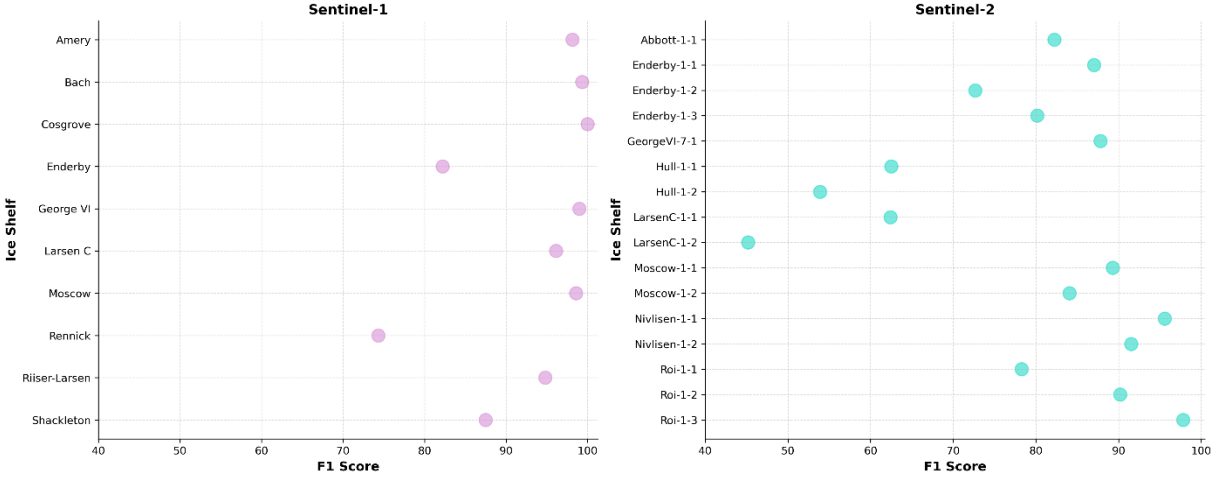

Figure 5 Accuracy assessment of the Sentinel-1 (left) and Sentinel-2 (right) supraglacial lake detection approaches. Data source: (Dirscherl et al., 2021a) and (Koehler et al., 2025).

https://doi.org/10.5194/essd-2025-569
Preprint. Discussion started: 12 May 2026

Open Access Earth System Science Data Discussions

280

Table 2 Lake detection accuracy based on precision, recall and F1-Score for Sentinel-1 and Sentinel-2 data. Data source: (Dirscherl et al., 2021a) and (Koehler et al., 2025).

Sentinel-1

Shelf	Precision	Recall	F1-Score
Larsen	0.99	0.93	0.96
Shack	1.00	0.78	0.88
Riiser	0.99	0.91	0.95
Moscow	0.98	0.99	0.99
Enderby	1.00	0.70	0.82
Cosgrove	1.00	1.00	1.00
Bach	0.99	0.99	0.99
Amery	0.96	1.00	0.98
George	0.99	0.99	0.99
Average	**0.99**	**0.92**	**0.95**

Sentinel-2

Shelf	Precision	Recall	F1 Score
Abbott-1-1	0.92	0.74	0.82
Enderby-1-1	0.85	0.89	0.87
Enderby-1-2	0.77	0.69	0.73
Enderby-1-3	0.85	0.76	0.80
GeorgeVI-7-1	0.85	0.91	0.88
Hull-1-1	0.81	0.51	0.63
Hull-1-2	0.89	0.39	0.54
LarsenC-1-1	0.58	0.68	0.62
LarsenC-1-2	0.31	0.85	0.45
Moscow-1-1	0.91	0.88	0.89
Moscow-1-2	0.79	0.90	0.84
Nivlisen-1-1	0.94	0.97	0.96
Nivlisen-1-2	0.90	0.93	0.92
Roi-1-1	0.87	0.71	0.78
Roi-1-2	0.88	0.92	0.90
Roi-1-3	0.98	0.97	0.98
Average	**0.91**	**0.91**	**0.91**

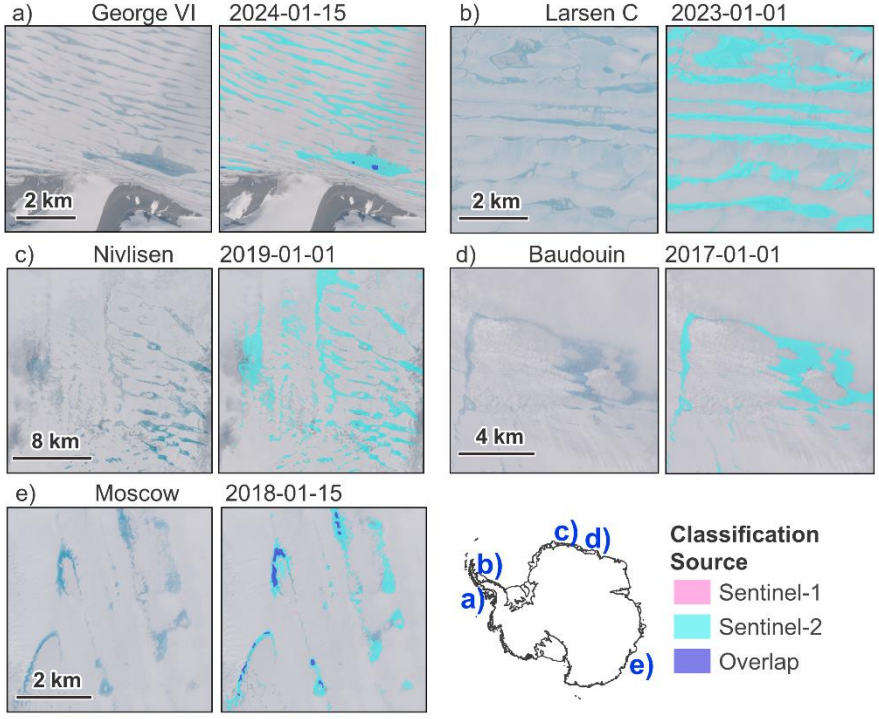

285 **Figure 6 Examples of bi-weekly maximum lake extents overlaid on the least-cloudy scene within each two-week period. The images demonstrate reliable lake detection despite thin cloud cover, primarily derived from optical Sentinel-2 imagery, with Sentinel-1 contributing minimally. Panel b) illustrates a minor overestimation under conditions of heavy slush.**

https://doi.org/10.5194/essd-2025-569
Preprint. Discussion started: 12 May 2026


Open Access Earth System Science Data Discussions

3.2 Lake detection confidence

Estimating uncertainty for supraglacial lake detection is challenging as accuracy for each bi-weekly maximum lake extent dataset depends on a number of factors such as general detection accuracy per shelf (which can vary strongly, e.g. Figure 5), scene availability, cloud coverage and lake surface conditions (e.g. refreezing, wind roughening). Most previous supraglacial lake studies do not provide uncertainty estimates (Arthur et al., 2022; Dell et al., 2024; Dirscherl et al., 2021a; Moussavi et al., 2020). One exception is the study by Mahagaonkar et al. (2024) providing uncertainties based on the scene availability during different melt stages with relative uncertainties relative to the melt peak resulting in a season based uncertainty. In contrast, this dataset provides temporally explicit confidence estimates for each bi-weekly lake extent product, thereby offering a more detailed and user-relevant characterization of data reliability compared to most existing studies.

The confidence metric is based on the availability of low-cloud Sentinel-2 observations (cloud cover < 25% from Level-2A products by European Space Agency), which represent the primary constraint on accurately mapping maximum lake extent. Rather than quantifying classification accuracy directly, the confidence estimate reflects the observational completeness of each bi-weekly composite. It therefore indicates the degree to which the mapped lake extent is supported by sufficient and unobstructed satellite observations Importantly, this metric does not quantify classification accuracy or provide a direct measure of areal uncertainty.

The confidence flag ranges from [-1, 1], where positive values indicate high observational coverage relative to the maximum number of low-cloud observations for a given ice shelf, and thus a high likelihood that the full lake extent has been captured. Negative values indicate reduced observational support due to limited scene availability. Low confidence values correspond to periods with limited suitable imagery and imply an increased likelihood of incomplete surface visibility, meaning that lake extents may be systematically underestimated. Consequently, reported lake areas with low confidence estimates should be interpreted as conservative estimates and usage of monthly or annual lake extent composites is encouraged. This provides users with critical context for assessing the reliability of spatial and temporal patterns in the dataset. Users can access this information via the corresponding <shelf-name>_stats_with_confidence_flag.csv files or directly through the lake extent plots, where confidence levels are visualized using a color scheme with blue colors for high confidence and orange colors for low confidence. As maximum lake extent typically occurs during peak melt conditions in January, the confidence of the annual maximum extent can be approximated by the confidence values of the corresponding January bi-weekly observations, with high confidence indicating a high likelihood that the annual extent is well captured.

https://doi.org/10.5194/essd-2025-569
Preprint. Discussion started: 12 May 2026

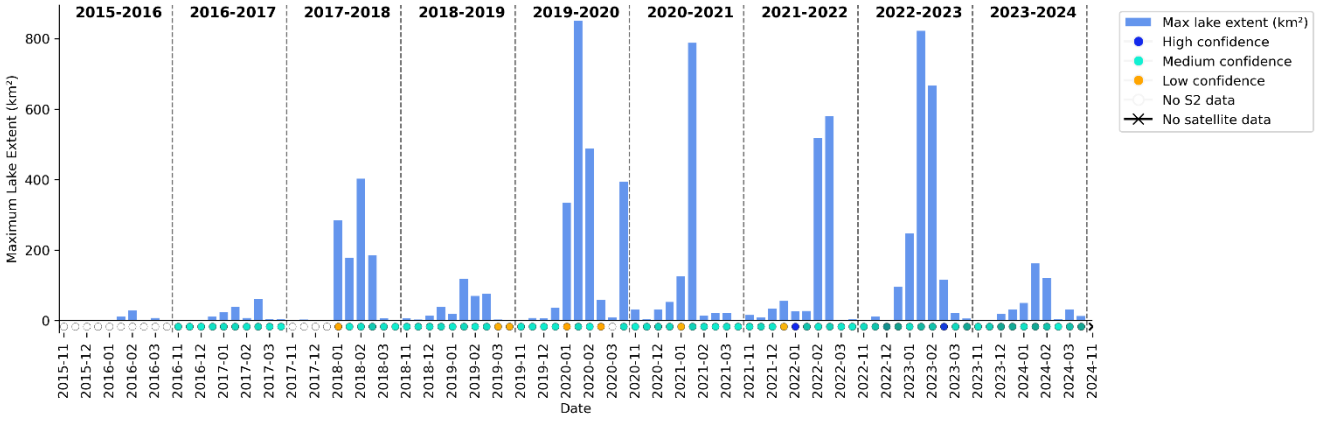

Figure 7 Bi-weekly supraglacial lake maximum extents on the George VI Ice Shelf with confidence indicators based on satellite data availability. Darker blue tones represent areas with sufficient cloud-free Sentinel-2 coverage, while turquoise indicates available scenes but with higher cloud occlusion. Orange tones denote insufficient cloud-free optical imagery, white indicates no available optical data at all, and black crosses mark regions with no satellite data coverage at all.

4 Dataset demonstration and limitations

This section illustrates a range of potential applications for the PolarLakes dataset while also acknowledging its inherent limitations. The examples focus on the analysis of pan-Antarctic supraglacial lake dynamics at a bi-weekly timescale, providing insights into the spatial and temporal patterns of surface water evolution. In particular, recurrence maps generated from bi-weekly observations reveal regions where supraglacial ponding occurs most frequently. Alongside these use cases, the section also outlines the constraints of the dataset, discussing aspects such as data quality, classification contribution from both sensors, and the types of analyses it can reliably support.

4.1 Pan-Antarctic bi-weekly supraglacial lake dynamics

Figure 8 illustrates the bi-weekly coverage of supraglacial lakes across Antarctica from all evaluated ice shelves between 2016 through 2024, limited to the period when both satellite sensors were operational. The intra-annual dynamics for each season closely resemble the same pattern for each melt period, with no significant differences among the various Antarctic regions. During the onset of melting in November and December, there are nearly no supraglacial lakes present. Starting in the second half of December, lake extents begin to steadily increase, reaching a maximum in the latter part of January. In February and March, the lake extent declines steadily to a minimum again. Deviations from this general pattern were noted in February 2022, when lake extents on the AP reached a maximum extent in the latter half of February rather than in January. This common pattern of inter-annual supraglacial lake dynamics was also found by various studies reporting a maximum of ponded meltwater in January due to the lower temporal resolution (Dell et al., 2024; Dirscherl et al., 2021b; Mahagaonkar et al., 2024). In contrast, the inter-annual lake extents vary much stronger between melt seasons. The largest area of pan-Antarctic supraglacial lakes was recorded in late January 2020, encompassing an area of 1924 square kilometers. The variations in the

https://doi.org/10.5194/essd-2025-569
Preprint. Discussion started: 12 May 2026

timing of maximum ponded areas are notably different across the distinct regions of the ice sheet. From 2017 through the peak year of 2020, the region occupied by supraglacial lakes on the EAIS was considerably greater than that on the AP. Following the pan-Antarctic peak in 2020, the ponding on East Antarctic ice shelves diminished while it increased on the shelves of the AP. A peak in the extent of supraglacial lakes was noted in 2023 over the AP resulting in even larger lake extents compared to the maximum in 2020 for the AP. Conversely, the WAIS has shown only limited extents of supraglacial lakes when compared to the EAIS and the AP. Nonetheless, West Antarctic ice shelves also experienced an overall lake extent peak in 2020, where the most extensive lake areas were documented. The least total area of pan-Antarctic lake extents was recorded during the 2024 melt season.

The distinct meltwater peak identified in 2020 is less significant when compared to previous research that highlights 2017 as the year with the greatest extent of supraglacial lakes. Most previous studies emphasize the melt season of 2017 as the most pronounced, with 2020 following closely behind (Arthur et al., 2022; Dell et al., 2024; Mahagaonkar et al., 2024). This observation can likely be linked to the availability of Landsat 8 and Sentinel-2 data during that period. Research utilizing Landsat-8 data indicates good coverage over Roi Baudouin in 2017, while 2020 had limited data availability. Conversely, the availability of Sentinel-2 images was quite restricted in 2017 but became adequate in 2020 according to our confidence assessment. Additionally, visual assessments reveal significant variation in the classification of lake versus slush over the Roi Baudouin Ice Shelf.

The investigations by Mahagaonkar et al. (2024) and Arthur et al. (2022) categorized extensive regions of the ice shelf as ponded,, while Dell et al. (2024) identified these areas as slush. The classification ruleset for the PolarLakes dataset (Baumhoer and Köhler, 2025) also regarded these regions as slush and are not included in the PolarLakes dataset. This discrepancy in the definition of lakes led to a substantial difference in the maximum lake extents recorded for the Roi Baudouin ice shelf. For instance, Mahagaonkar et al. (2024) reported areas reaching up to 600 square kilometers, whereas this study indicates a maximum extent of 287 square kilometers for Roi Baudouin. The Roi Baudouin Ice Shelf ranks third in terms of lake area, following the Amery Ice Shelf and George VI Ice Shelf, thus significantly impacting pan-Antarctic statistics. Furthermore, Arthur et al. (2022) emphasize that the high point noted in 2017 correlates with notable irregularities in the Amery and Roi Baudouin ice shelves. Ignoring these irregularities, Arthur et al. (2022) also identify the highest lake extent in 2020.

https://doi.org/10.5194/essd-2025-569
Preprint. Discussion started: 12 May 2026

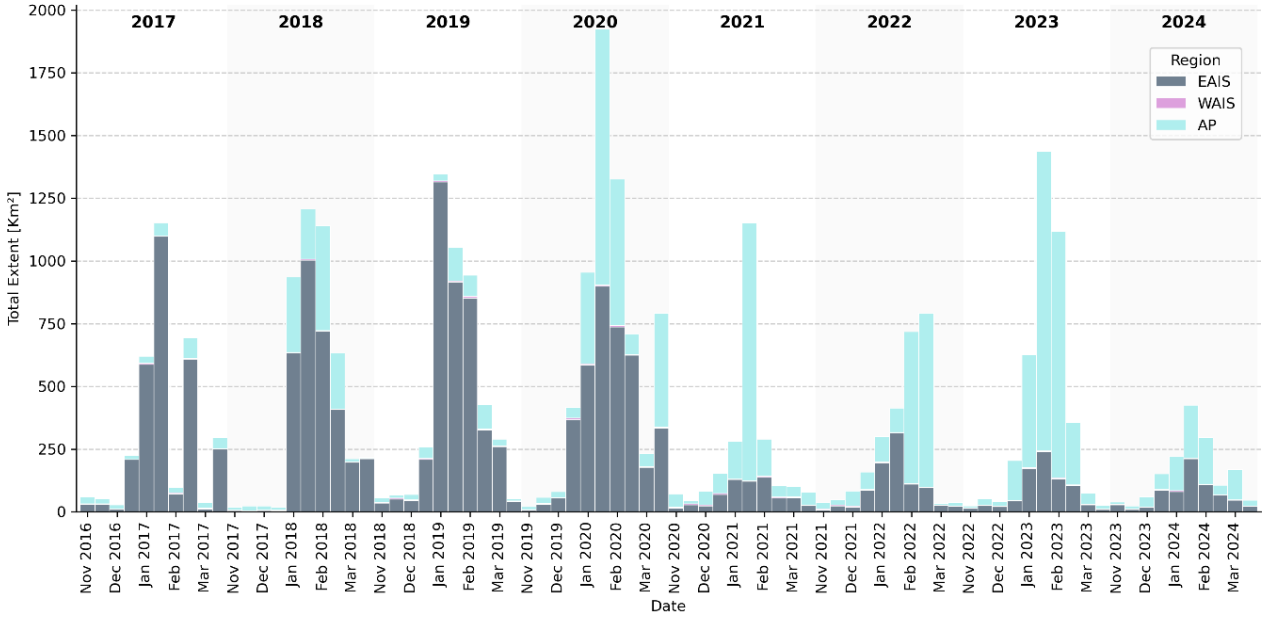

Figure 8 Cumulated bi-weekly supraglacial lake extents over Antarctica separated by regions for the Antarctic Peninsula (AP), West Antarctic Ice Sheet (WAIS) and East Antarctic Ice Sheet (EAIS).

4.2 Recurrence maps

The PolarLakes recurrence dataset for the full observation timeframe is illustrated in Figure 9, featuring six representative ice shelves. The occurrence of supraglacial lakes exhibits significant variability from one year to the next and varies independently for each ice shelf. Note that the recurrences were calculated over different time periods (e.g. Larsen C starting from November 2014 and Baudouin from Nov 2016 onwards), hence, the maximum potentially possible recurrence time can vary. The Amery Ice Shelf records the highest recurrence rates at 42 instances, followed by the Bach and George VI ice shelves with 38 and 35 bi-weekly occurrences, respectively. On the Bach Ice Shelf, supraglacial lakes are primarily located near the grounding line, with the most significant concentrations found in local ice-surface depressions. Similarly, on the George VI Ice Shelf, the recurrence of supraglacial lakes is greater in regions near the grounding line, adjacent to rock outcrops, as well as on the shelf in stream-like local depressions.

https://doi.org/10.5194/essd-2025-569
Preprint. Discussion started: 12 May 2026

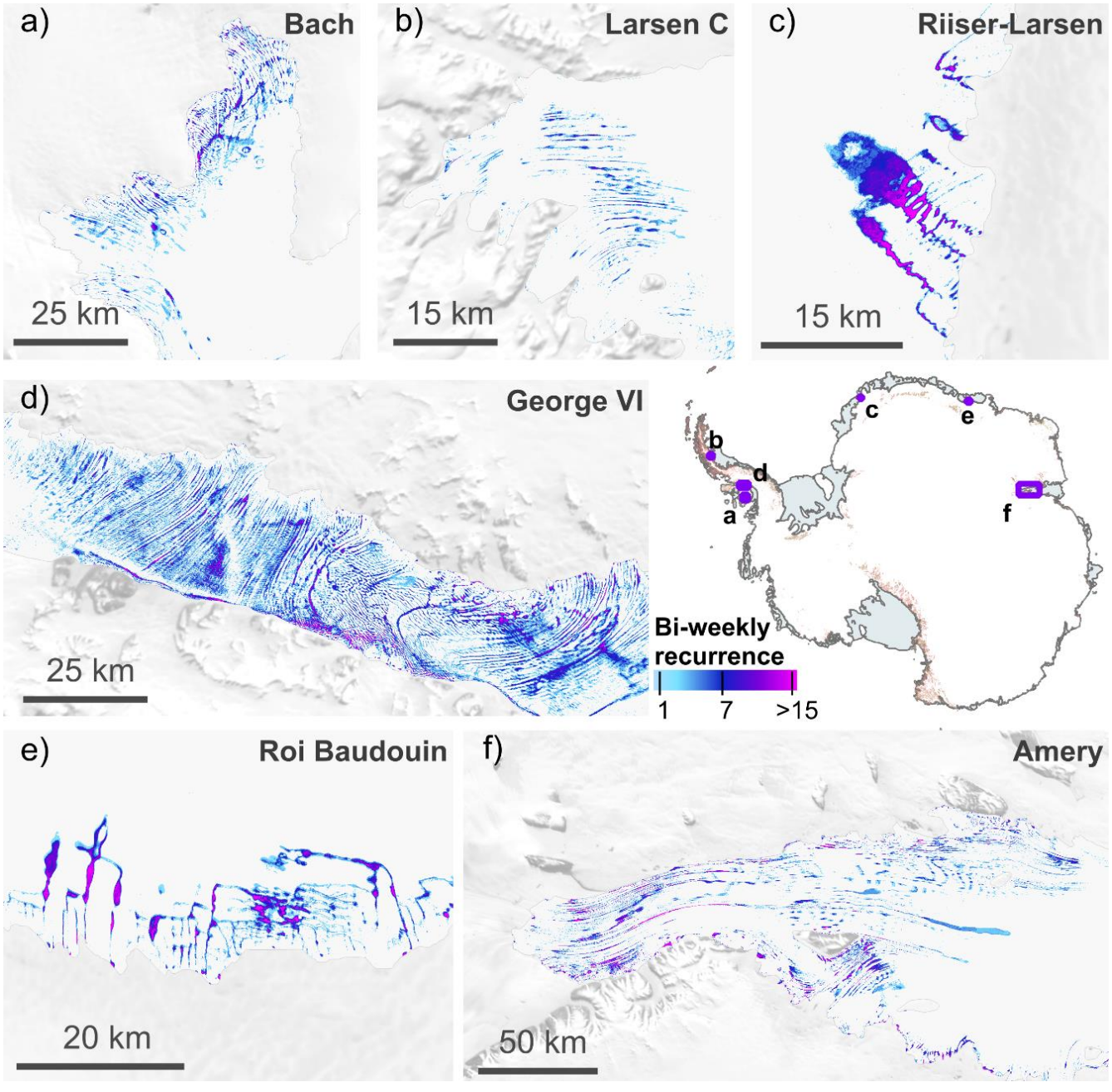

Figure 9 Bi-weekly recurrence of supraglacial lakes during austral summer (November until March) for (a) Bach Ice Shelf (2015-2024), (b) Larsen C Ice Shelf (2014-2024), (c) Riiser-Larsen Ice Shelf (2016-2024), (d) George VI Ice Shelf (2015-2024), (e) Baudouin Ice Shelf (2016-2024), and (f) Amery Ice Shelf (2015-2024).

The supraglacial lakes on the Amery and Roi Baudouin ice shelves display a comparable spatial distribution, with lakes situated near the grounding line where rock outcrops and blue ice regions are present. Lakes exhibiting the highest recurrence frequencies typically form in local depressions. Ponding on the flat ice shelf occurs only in years with substantial surface

https://doi.org/10.5194/essd-2025-569
Preprint. Discussion started: 12 May 2026

melting, yet it still adheres to local depressions and flow lines. Conversely, the Riiser-Larsen and Larsen C ice shelves face significantly lower recurrence rates, recording 18 and 14 instances, respectively. This shows the differences in ponding throughout the AP and the EAIS, where ponding was either pronounced in the first half until 2020 or the second afterwards, but not throughout the whole observation timeframe. The Riiser-Larsen Ice Shelf saw regular ponding until 2020, with nearly no lake area observed afterwards. In contrast, the Larsen C Ice Shelf began to exhibit extensive supraglacial lake formations following the pan-Antarctic maximum in 2020, reaching its peak in 2023.

4.3 Limitations

The analysis presented in this study is subject to several limitations that must be acknowledged. Firstly, the time series data utilized is only consistent from the melt season of 2016-2017 onwards, as it relies on the availability of both Sentinel-1 and Sentinel-2 sensors. Consequently, the fraction of lake extents detected solely from Sentinel-1 data is significantly smaller compared to the fused product from both sensors. This discrepancy suggests that for consistency, it may be more appropriate to consider the PolarLakes dataset exclusively from 2016-2017 onwards for time series analysis. The assessment of lake surface area using Sentinel-1 alone, often falls short of accurately representing the true maximum lake area as exemplified in Figure 10 for Moscow University Ice Shelf. Hence, it is important to consider the confidence estimate if there is a notable difference in maximum lake area between two phases of significant lake extents. In instances of low confidence, this area estimate is likely to be less than the actual lake extent due to the limited availability of cloud free Sentinel-2 satellite data.

Moreover, the choice of Sentinel-2 images relies on cloud coverage, and the confidence estimates are calculated based on the given cloud cover value. It is recognized that there are inaccuracies in cloud cover detection in polar regions, particularly over the Antarctic ice sheet, which may lead to misclassification of satellite scenes. This can result in the exclusion of truly cloud-free scenes and the inclusion of heavily clouded scenes during the classification process. Besides, significant errors can arise from high cloud cover and the presence of cloud shadows, as these shadows may be incorrectly identified as lakes. To address this problem, we limited our analysis to regions that were detected more than two times throughout the entire time series (Dell et al., 2024). However, this method may still cause a slight decrease in the identified maximum lake extent by a few pixels at the edges of lakes that have only achieved their maximum extent once. This reduction is not substantial, as during particularly large lake extents, the lakes typically persist for longer durations, and our bi-weekly dataset captures them more frequently than twice due to its high temporal resolution. Finally, providing precise uncertainty values for the identified lake extents is complicated by various factors, such as detection accuracy per shelf and the cloud coverage in Sentinel-2 data. Although we offer confidence assessments for each bi-weekly maximum lake extent based on the availability of cloud-free optical data and a comprehensive accuracy analysis for lake detection utilizing optical and SAR data, the cumulative uncertainties related to each specific ice shelf tied to every bi-weekly lake extent estimation still pose a challenge for this study.

https://doi.org/10.5194/essd-2025-569
Preprint. Discussion started: 12 May 2026

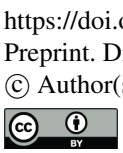

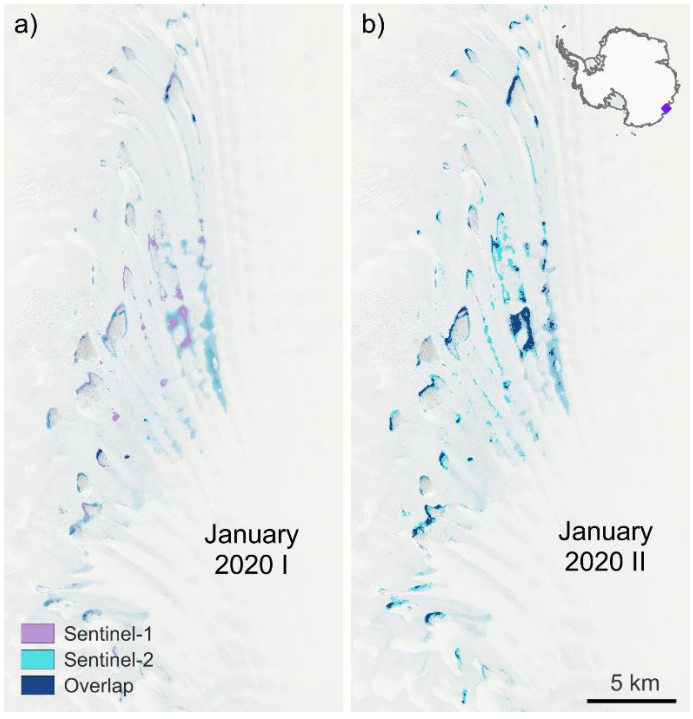

Figure 10 Example of classification sources during periods of heavy cloud cover over the Moscow University Ice Shelf. (a) During heavy cloud cover (median cloud cover of 84 %) during the first half of January 2020, 91 % of the lake area was classified using Sentinel-1 imagery, shown in purple. (b) During the second half of January, when the median cloud cover was 30 %, larger lake extents were classified using Sentinel-2 imagery (turquoise). Overall, 38 % of the lake area was classified using both image sources (dark blue). Copernicus Sentinel-2 Data 2025.

5 Dataset Availability

The PolarLakes dataset is available at https://geoservice.dlr.de/web/datasets/polarlakes (Baumhoer et al., 2025) providing bi-weekly maximum extents of supraglacial lakes on 22 major Antarctic ice shelves. The dataset covers the melt period between November and March during austral summer over the entire Sentinel era. Depending on satellite data availability, the PolarLakes dataset starts in the melt period 2015-2016 for most ice shelves based on Sentinel-1 data only. From the melt season 2016-2017 onwards the dataset is based on Sentinel-1 and Sentinel-2 data. The PolarLakes data is provided in three different folders at a gridded spatial resolution of 10 meters. The bi-weekly maximum extents are stored in the folder *<shelfname>_biweekly_mosaics*. The binary maximum extent raster files are named *yyyy-mm-01_max_extent.tif* for the first half of the month (until 15th) and *yyyy-mm-16_max_extent.tif* for the second half of the month. The second folder *<shelfname>_annual_mosaics* includes annual and total recurrence raster files. Based on the bi-weekly maximum extents we calculated the annual recurrence indicating how many times the lake was detected during the season with the possible maximum of 10 times. The annual recurrence mosaics are named *sum_<startyear>-11-01_<endyear>-03-31_<shelfname>.tif*. The folder for annual mosaics also includes a total recurrence raster *total_<startyear>-11-*

https://doi.org/10.5194/essd-2025-569
Preprint. Discussion started: 12 May 2026

01_<endyear>-03-31_<shelfname>.tif indicating the number of times a lake occurred based on a bi-weekly basis over the entire available observation time for each ice shelf (hence, the maximum possible recurrence varies). In the folder *<shelfname>_stats_plots*, the PolarLakes dataset also provides a plot of bi-weekly maximum lake extents with quality flag for each ice shelf (similar to Figure 7), a satellite sensor contribution plot with information about median cloud cover (similar to Figure 4), and a table with bi-weekly maximum lake extents, quality value, satellite sensor contribution percentage and, extended cloud cover statistics. Table 3 summarizes the temporal coverage for each ice shelf as well as the number of Sentinel-1 and Sentinel-2 scenes used for generating the dataset. In total, the PolarLakes dataset is based on 20,250 Sentinel-1 and 25,772 Sentinel-2 scenes. Besides the PolarLakes dataset we also published the ruleset on labelling supraglacial lakes in optical data and the resulting labels to train the model for Sentinel-2 data at https://doi.org/10.5281/zenodo.15723722. The code used to produce the PolarLakes dataset and figures for this publication is also made available at https://doi.org/10.5281/zenodo.17467230. The code incorporates Jupyter Notebook examples, which illustrate the methodology of training the U-Net on proprietary data, and the subsequent execution of inference based on pre-trained weights that have been produced for this publication.

Table 3 Numbers of Sentinel-1 and Sentinel-2 input scenes over all investigated ice shelves including the start and end date of the temporal coverage. RDW: Robert/Downer/Wilma.

Ice Shelf	Start	End	S1 Scenes	S2 Scenes	All Scenes
Abbot	2014	2024	2222	937	3159
Amery	2015	2024	1730	4472	6202
Bach	2015	2024	1462	1614	3076
Baudouin	2016	2024	1144	1940	3084
George VI	2015	2024	1742	3097	4839
Hull	2016	2024	256	186	442
LarsenC	2014	2024	2996	1852	4848
LarsenD	2015	2024	1558	1940	3498
Moscow	2016	2024	556	386	942
Mulebreen	2016	2024	498	332	830
Nickerson	2016	2024	822	488	1310
Nivlisen	2016	2024	492	1200	1692
Pine Island	2016	2024	0	226	226
Publications	2015	2024	432	291	723
Ranvik	2015	2024	246	74	320
Rayner	2015	2024	162	1134	1296
Riiser-Larsen	2016	2024	318	1245	1563
RDW	2016	2024	500	453	953
Shackleton	2016	2024	536	1072	1608
Sulzberger	2016	2024	1102	1228	2330
Utsikkar	2015	2024	356	289	645
Wilkins	2015	2024	1120	1316	2436
Total			**20250**	**25772**	**46022**

https://doi.org/10.5194/essd-2025-569
Preprint. Discussion started: 12 May 2026

6 Conclusions

The PolarLakes dataset offers a comprehensive bi-weekly overview of supraglacial lake dynamics across 22 individual ice shelves, which is a significant advancement in understanding pan-Antarctic supraglacial lake behaviors. Covering an extensive period from 2015 through 2024, this dataset not only extends existing research but also integrates both optical and SAR satellite data for improved supraglacial lake mapping. Our findings reveal that the extents of supraglacial lakes were notably larger in East Antarctica from 2016 through 2020, culminating in a pan-Antarctic maximum in 2020. However, in the more recent period, we noted a considerable decline of ponding in East Antarctica. This is in contrast to the AP, where extensive lake areas persisted and reached another peak in lake extent in 2023. The PolarLakes dataset provides new insights into supraglacial lake dynamics, facilitated by its longer temporal coverage and higher temporal resolution. Such detailed observations are crucial for advancing our understanding of the hydrological processes on the Antarctic ice shelves. The dataset presented here provides a valuable observational resource for improving hydrological surface models and for advancing understanding of the role of supraglacial lake dynamics in modulating ice-shelf stability and, ultimately, ice-sheet dynamics.

Supplement

Author contributions

Conceptualization: C.B.; A.D.; C.K. Data curation: C.B; J.K. Formal Analysis: C.B. Funding Acquisition: A.D. Investigation: C.B. Methodology: C.B.; J.K. Project administration: C.B.; A.D. Software: C.B.; J.K. Supervision: C.K.; B.W.; S.L.; Validation: C.B.; J.K. Visualization: C.B. Writing - original draft: C.B. Writing – Review & Editing: C.K.; J.K.; B.W..; A.D. All authors approved the final submitted draft.

Acknowledgements

The authors acknowledge the European Space Agency and the European Commission for the acquisition and availability of Copernicus Sentinel-1 and Sentinel-2 data. Furthermore, the authors thank the Antarctic Digital Database for providing the high-resolution coastline dataset version 7.10 open access.

The authors used DeepL Write and SciSpace to enhance the style of the pre-written text of this manuscript and correct grammatical errors. The tools were not used to generate new text, content or citations, nor to summarise other existing works. The authors used Copilot, which runs on Sonnet 4.5 and Claude Haiku 4.5 models, to improve the structure of the code and add extensive documentation to enhance reproducibility. After applying these tools, the authors carefully checked the results and tested the code, taking full responsibility for the final version.

Competing interests

The authors declare no conflicts of interest.

Financial support

This work was supported by the European Space Agency (ESA) under Contract No. 4000141701/23/I-DT-bgh within the framework of the "Future EO-1 EO Science for Society Permanently Open Call" and the Polar Monitor Project (DLR).

References

Antarctic Digital Database: https://www.add.scar.org/, last access: 3 February 2020.

Arthur, J. F., Stokes, C., Jamieson, S. S., Carr, J. R., and Leeson, A. A.: Recent understanding of Antarctic supraglacial lakes using satellite remote sensing, Progress in Physical Geography: Earth and Environment, 44, 837–869, https://doi.org/10.1177/0309133320916114, 2020.

Arthur, J. F., Stokes, C. R., Jamieson, S. S. R., Rachel Carr, J., Leeson, A. A., and Verjans, V.: Large interannual variability in supraglacial lakes around East Antarctica, Nat Commun, 13, 1711, https://doi.org/10.1038/s41467-022-29385-3, 2022.

Baumhoer, C. and Köhler, J.: Training, testing and intercomparison data for the segmentation of supraglacial lakes in Antarctica, https://doi.org/10.5281/zenodo.15723722, 2025.

Baumhoer, C., Koehler, J., Dietz, A. J., and Kuenzer, C.: PolarLakes - Bi-weekly supraglacial lake dynamics in Antarctica, DLR (v1), https://doi.org/10.15489/uiusp1di1i62, 2025.

Baumhoer, C. A., Dietz, A. J., Heidler, K., and Kuenzer, C.: IceLines – A new data set of Antarctic ice shelf front positions, Sci Data, 10, 138, https://doi.org/10.1038/s41597-023-02045-x, 2023.

Bell, R. E., Banwell, A. F., Trusel, L. D., and Kingslake, J.: Antarctic surface hydrology and impacts on ice-sheet mass balance, Nature Climate Change, 1, https://doi.org/10.1038/s41558-018-0326-3, 2018.

Corr, D., Leeson, A., McMillan, M., Zhang, C., and Barnes, T.: An inventory of supraglacial lakes and channels across the West Antarctic Ice Sheet, Earth System Science Data, 14, 209–228, https://doi.org/10.5194/essd-14-209-2022, 2022.

Dell, R. L., Banwell, A. F., Willis, I. C., Arnold, N. S., Halberstadt, A. R. W., Chudley, T. R., and Pritchard, H. D.: Supervised classification of slush and ponded water on Antarctic ice shelves using Landsat 8 imagery, Journal of Glaciology, 68, 401–414, https://doi.org/10.1017/jog.2021.114, 2022.

Dell, R. L., Willis, I. C., Arnold, N. S., Banwell, A. F., and de Roda Husman, S.: Substantial contribution of slush to meltwater area across Antarctic ice shelves, Nat. Geosci., 1–7, https://doi.org/10.1038/s41561-024-01466-6, 2024.

Dirscherl, M., Dietz, A. J., Kneisel, C., and Kuenzer, C.: Automated Mapping of Antarctic Supraglacial Lakes Using a Machine Learning Approach, Remote Sensing, 12, 1203, https://doi.org/10.3390/rs12071203, 2020.

Dirscherl, M., Dietz, A. J., Kneisel, C., and Kuenzer, C.: A Novel Method for Automated Supraglacial Lake Mapping in Antarctica Using Sentinel-1 SAR Imagery and Deep Learning, Remote Sensing, 13, 197, https://doi.org/10.3390/rs13020197, 2021a.

Dirscherl, M., Dietz, A. J., and Kuenzer, C.: Seasonal evolution of Antarctic supraglacial lakes in 2015–2021 and links to environmental controls, The Cryosphere, 15, 5205–5226, https://doi.org/10.5194/tc-15-5205-2021, 2021b.

https://doi.org/10.5194/essd-2025-569
Preprint. Discussion started: 12 May 2026

Dirscherl, M. C.: Remote Sensing of Supraglacial Lake Dynamics in Antarctica - Exploiting Methods from Artificial Intelligence for Derivation of Antarctic Supraglacial Lake Extents in Multi-Sensor Remote Sensing Data, Universität Würzburg, https://doi.org/10.25972/OPUS-27950, 2022.

Feyisa, G. L., Meilby, H., Fensholt, R., and Proud, S. R.: Automated Water Extraction Index: A new technique for surface water mapping using Landsat imagery, Remote Sensing of Environment, 140, 23–35, https://doi.org/10.1016/j.rse.2013.08.029, 2014.

Fürst, J. J., Durand, G., Gillet-Chaulet, F., Tavard, L., Rankl, M., Braun, M., and Gagliardini, O.: The safety band of Antarctic ice shelves, Nature Climate Change, 6, 479–482, 2016.

Koehler, J., Baumhoer, C., Wouters, B., Lhermitte, S., and Dietz, A.: Advancing Supraglacial Lake Mapping in Antarctica: A Deep Learning Approach Using Sentinel-2 Imagery, https://doi.org/10.33774/coe-2025-6svt4, 8 September 2025.

Lai, C.-Y., Kingslake, J., Wearing, M. G., Chen, P.-H. C., Gentine, P., Li, H., Spergel, J. J., and van Wessem, J. M.: Vulnerability of Antarctica's ice shelves to meltwater-driven fracture, Nature, 584, 574–578, https://doi.org/10.1038/s41586-020-2627-8, 2020.

Leeson, A. A., Forster, E., Rice, A., Gourmelen, N., and Van Wessem, J. M.: Evolution of Supraglacial Lakes on the Larsen B Ice Shelf in the Decades Before it Collapsed, Geophysical Research Letters, 47, e2019GL085591, https://doi.org/10.1029/2019GL085591, 2020.

Mahagaonkar, A., Moholdt, G., Glaude, Q., and Schuler, T. V.: Supraglacial lake evolution and its drivers in Dronning Maud Land, East Antarctica, J. Glaciol., 1–15, https://doi.org/10.1017/jog.2024.66, 2024.

Mellor, M. and McKinnon, G.: The Amery Ice Shelf and its hinterland, Polar Record, 10, 30–34, https://doi.org/10.1017/S0032247400050579, 1960.

Moussavi, M., Pope, A., Halberstadt, A. R. W., Trusel, L. D., Cioffi, L., and Abdalati, W.: Antarctic Supraglacial Lake Detection Using Landsat 8 and Sentinel-2 Imagery: Towards Continental Generation of Lake Volumes, Remote Sensing, 12, 134, https://doi.org/10.3390/rs12010134, 2020.

Sen2Cor 2.11.00 Software Release Note: https://step.esa.int/thirdparties/sen2cor/2.11.0/docs/OMPC.TPZG.SRN.003%20-%20i1r0%20-%20Sen2Cor%202.11.00%20Software%20Release%20Note.pdf.

Scambos, T. A., Hulbe, C., Fahnestock, M., and Bohlander, J.: The link between climate warming and break-up of ice shelves in the Antarctic Peninsula, Journal of Glaciology, 46, 516–530, https://doi.org/10.3189/172756500781833043, 2000.

Scambos, T. A., Bohlander, J. A., Shuman, C. A., and Skvarca, P.: Glacier acceleration and thinning after ice shelf collapse in the Larsen B embayment, Antarctica, GEOPHYSICAL RESEARCH LETTERS, 31, https://doi.org/10.1029/2004GL020670}, 2004.

SNAP: SNAP - ESA Sentinel Application Platform, version 8.0.5, 2020.

Stokes, C. R., Sanderson, J. E., Miles, B. W. J., Jamieson, S. S. R., and Leeson, A. A.: Widespread distribution of supraglacial lakes around the margin of the East Antarctic Ice Sheet, Sci Rep, 9, 13823, https://doi.org/10.1038/s41598-019-50343-5, 2019.

Trusel, L. D., Frey, K. E., Das, S. B., Karnauskas, K. B., Kuipers Munneke, P., Van Meijgaard, E., and Van Den Broeke, M. R.: Divergent trajectories of Antarctic surface melt under two twenty-first-century climate scenarios, Nature Geosci, 8, 927–932, https://doi.org/10.1038/ngeo2563, 2015.

https://doi.org/10.5194/essd-2025-569
Preprint. Discussion started: 12 May 2026

Tuckett, P. A., Ely, J. C., Sole, A. J., Livingstone, S. J., Davison, B. J., Melchior van Wessem, J., and Howard, J.: Rapid accelerations of Antarctic Peninsula outlet glaciers driven by surface melt, Nat Commun, 10, 4311, https://doi.org/10.1038/s41467-019-12039-2, 2019.

Wessel, B., Huber, M., Wohlfart, C., Bertram, A., Osterkamp, N., Marschalk, U., Gruber, A., Reuß, F., Abdullahi, S., Georg, I., and Roth, A.: TanDEM-X PolarDEM 90 of Antarctica: generation and error characterization, The Cryosphere, 15, 5241–5260, https://doi.org/10.5194/tc-15-5241-2021, 2021.